



computational proteomics

## Laboratory for Computational Proteomics

[www.FenyoLab.org](http://www.FenyoLab.org)

E-mail: [Info@FenyoLab.org](mailto:Info@FenyoLab.org)

Facebook: [\*NYUMC Computational Proteomics Laboratory\*](#)

Twitter: [\*@CompProteomics\*](#)

## On the ejection of hydrogen ions from organic solids impacted by MeV ions

D. Fenyö, P. Håkansson and B.U.R. Sundqvist

*Division of Ion Physics, Dept. of Radiation Sciences, Uppsala University, Box 535, S-751 21 Uppsala, Sweden*

Received 23 April 1993 and in revised form 27 July 1993

In the ejection of material from organic solids following MeV ion bombardment, the initial velocities of the ejected species contain information on their interaction at the surface of the solid and the seldge. Here, experimental data are presented on the sample thickness dependence of the yield (the number of secondary ions per incoming ion) and the initial radial velocity distribution of singly charged hydrogen ions ( $H^+$ ,  $H_2^+$ ,  $H_3^+$ ,  $H^-$ ) and other low-mass fragments ejected from organic solids of nitrocellulose and arachidic acid due to the impact of 72.3 MeV  $^{127}I^{14+}$  ions. An increase is observed in the width of the radial velocity distribution of the positive hydrogen ions as the thickness of the nitrocellulose film is increased. The results are in qualitative agreement with simulations based on Coulomb repulsion from the charged track created by the incident ion.

### 1. Introduction

A fast heavy ion ( $\sim 1$  MeV/u) penetrating an organic solid causes ejection of secondary ions and neutrals from the solid [1]. A description of the mechanism of the formation and ejection of secondary ions does not exist, even for the case of the lightest and least complex of the ions observed, the hydrogen ions  $H^+$ ,  $H_2^+$ ,  $H_3^+$  and  $H^-$ . The purpose of this paper is to present experimental data and a simple calculation that contribute to an understanding of the ejection process of these low-mass species, which are an important part of the mass spectrum even when the goal is the study of biomolecules [3].

The origin of the hydrogen ions is uncertain at present. Possible sources include: the organic sample molecules; surface contaminant molecules like pump oil with a high hydrogen content, and adsorbed hydrogen-containing molecules. Positive hydrogen ions can be created by several mechanisms, including: direct ionization by the primary ion; repulsive decay of electronically excited molecules; and gas phase collisions between ejected atoms and molecules.  $H^-$  can be formed by low energy electron capture [4].

The location of the origin of the light ion species has been examined by studying the yield dependence on the parameters of the incident ion beam such as mass and charge state. As a function of the primary ion charge state ( $q$ ) the yield of  $H^+$  varies as  $q^n$ , with

$n \approx 3$  [5]. For a constant primary ion velocity and charge state the yield of  $H^+$  is independent of the mass of the projectile unlike the yield of heavier secondary ions. This means that only the energy lost by the primary ion near the sample surface contributes to the ejection of  $H^+$ , because incident ions with different mass will reach different equilibrium charge states and thus have different stopping power deeper inside the sample. For heavier secondary ions, on the other hand, the energy deposited at depths for which the charge state has changed considerably from the initial also contributes to the ejection. From this it is concluded that  $H^+$  is created close to the surface and is ejected from the solid earlier than heavier secondary ions [5].

The axial component of the energies of desorbed particles also gives useful information about the desorption mechanism. It has been established that  $H^+$  and  $H_2^+$  have higher mean *axial* energies than the heavier secondary ions [6–12]. Furthermore, their *axial* energies are thickness dependent [8]. To account for this effect it has been proposed that the secondary ions are accelerated due to the Coulomb interaction with the short-lived *infra* track of positive ions created by the primary ion [8,10]. The velocity distribution of the positive hydrogen ions should be affected more than that of other secondary ions because  $H^+$  is created closer to the ion path and ejected at earlier times than other more massive secondary ions.

In this paper measurements are presented on the sample thickness dependence of the yield and the initial *radial* velocity distribution of charged hydrogen ions ejected from organic solids due to the impact of

*Correspondence to:* D. Fenyö, Rockefeller University, 1230 York Avenue, New York, NY 10021, USA.

MeV ions. The data are compared with results of computer simulations of the desorption process based on the Coulomb repulsion model. The results indicate that the hydrogen ions sample the transient Coulomb repulsion from the track of positive charges created by the primary ion and are neutralized by electrons from the substrate.

## 2. Experimental

The organic samples studied include nitrocellulose, which is a polymer employed in biochemistry for protein adsorption, and arachidic acid, which is an amphipatic linear fatty acid. Thin films of nitrocellulose (0–800 Å) and arachidic acid (0–350 Å) were prepared on silicon backings using the spin coating method [13], in which a droplet of solution containing the sample is applied to the rotating substrate. Langmuir–Blodgett films of arachidic acid molecules were also prepared according to a known procedure [14]. First, a submonolayer coverage of arachidic acid molecules is formed on a water surface. Next, the arachidic acid overlayer is compressed to form a monolayer coverage. Finally, several layers are transferred to a clean etched silicon substrate yielding a film with a well-defined structure. The thickness of the films was determined by ellipsometry [15] for both deposition techniques. The surface roughness of the spin-coated films was measured to be less than 50 Å by atomic force microscopy [16].

Either fission fragments from a  $^{252}\text{Cf}$  source or 72.3 MeV  $^{127}\text{I}^{14+}$  ions from the tandem accelerator at The Svedberg Laboratory in Uppsala were used as primary ions. The ions bombard the sample at an angle of incidence of  $45^\circ$ . A pressure of  $10^{-6}$  Torr is maintained in the experimental chamber. The secondary ions ejected upon primary ion impact are identified by time-of-flight mass spectrometry [17]. The lower mass region of a typical time-of-flight spectrum of positive

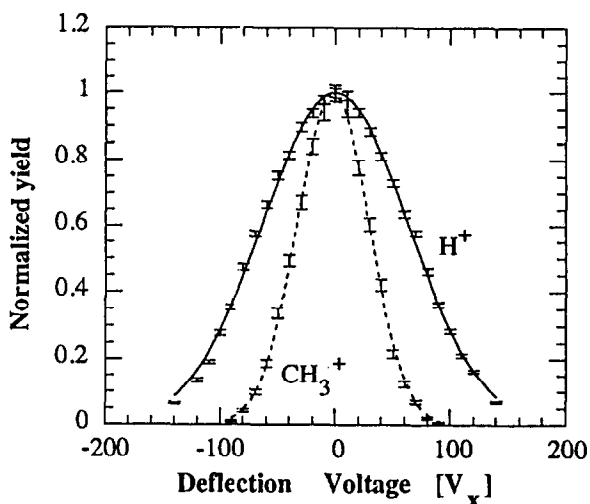


Fig. 2. The yield of  $\text{H}^+$  and  $\text{CH}_3^+$  ions from a nitrocellulose sample as a function of the deflection voltage.

secondary ions ejected as a result of ion impact is presented in fig. 1. The distribution of the component of the velocity along the  $x$ -axis (referred to as the radial velocity in the following presentation) was determined by measuring the secondary ion yield as a function of the voltage applied to a pair of deflection plates (fig. 2). The velocity was calculated from the deflection voltage as described elsewhere [18]. The mean kinetic energy was calculated by a least-squares fit of a Gaussian to the experimental radial velocity distribution and correcting for the instrumental broadening.

## 3. Simulations

If the net positive charge of the infra track, created by the primary ion in the solid, survives for a sufficiently long time, the electric field resulting therefrom

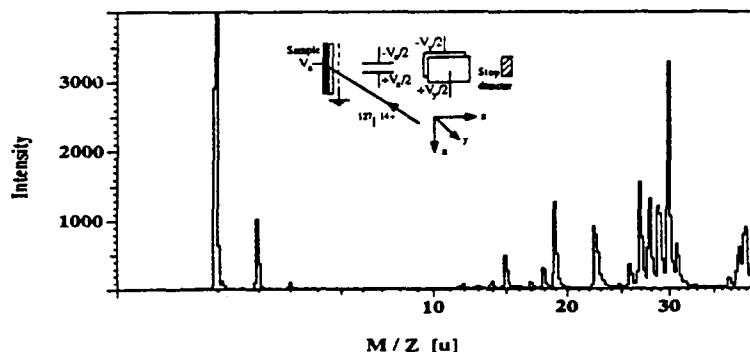


Fig. 1. An example of a time of flight spectrum of low mass positive ion ejecta from a nitrocellulose sample due to the impact of 72.3 MeV  $^{127}\text{I}^{14+}$  ions. The inset shows a schematic of the experimental setup.

could influence the velocity distribution of ejected ions. This was the conclusion based on the experimental observation that a thin layer of gold on top of nitrocellulose reduces the mean *axial* energy of the ejected  $H^+$  [10] and that the *axial* velocity changes with sample thickness [8]. Here we will use this concept to study the change in the radial velocity distribution. That is, Monte Carlo simulations are performed on the influence of a cylindrical charge distribution on the velocity distribution of ejected  $H^+$ . It is assumed that the primary ion creates a cylindrical track of homogeneously distributed positive point charges within a distance of one Bohr adiabatic radius ( $2.5 \text{ \AA}$  for  $72.3 \text{ MeV } ^{127}\text{I}$ ) from the path of the incident ion. The charge density is calculated from the electronic stopping power ( $820 \text{ eV/\AA}$  for  $72.3 \text{ MeV } ^{127}\text{I}$  in nitrocellulose) using the average energy to create an electron-hole pair as a parameter. It is determined to be  $50 \text{ eV}$ , a value somewhat larger than is typically used for the bulk, by fitting the width of the simulated radial velocity distribution of hydrogen ions to that experimentally obtained for the thickest nitrocellulose film used. The electric field was calculated under the assumptions that the solid has a plane surface and was characterized by its dielectric constant,  $\epsilon_r \approx 7$  [19]. Although the dielectric constant of the charged track is expected to be lower than the bulk value because it will be more difficult to polarize due to the lack of loosely bound electrons, this was not taken into account. Finally the charged track was assumed to have a time dependent charge density ( $q = q_0 e^{-t/\tau}$ ), where  $\tau$  is called the neutralization time.

It is assumed that  $H^+$  is created inside the charged track, homogeneously distributed from the surface

down to a maximal depth. If  $H^+$  is only ejected from the sample surface the angular distribution shows an alignment along the axis of the charged track. If  $H^+$  is ejected from deep down in the sample, on the other hand, the ejection perpendicular to the axis of the charged track will be favored. The maximal depth from which  $H^+$  can be ejected is chosen to be  $5 \text{ \AA}$  in order to give radial velocity distributions for  $45^\circ$  angle of incidence which are in agreement with experimental data on  $H^+$  from nitrocellulose films bombarded with fast iodine ions, i.e. the radial velocity distribution corresponds to ejection on the average in a direction normal to the surface [18]. It is assumed that  $H^+$  is created in a dissociation of a sample molecule to account for the energy acquired in such a process an initial kinetic energy of  $4 \text{ eV}$  in an arbitrary direction of motion was given to the hydrogen ions [20].

Ejected ions can be neutralized through electron capture. The main source of electrons is the sample and therefore the neutralization probability of ejected ions will depend on their escape velocity [21]. This was taken into account by applying a velocity dependent survival probability,  $p \propto \exp(-v_0/v_z)$ , where  $v_z$  is the component of the velocity normal to the surface [22]. The constant  $v_0$  was determined to be  $4 \times 10^4 \text{ m/s}$  by a fit of the width of the simulated radial velocity distribution of hydrogen ions to that experimentally obtained for the bare silicon substrates.

Calculations were performed on the classical trajectories of the hydrogen ions as they were accelerated by repulsion from the charged track varying the track length and the neutralization time of the charged track. For each thickness the trajectories of 20 000 particles were calculated.

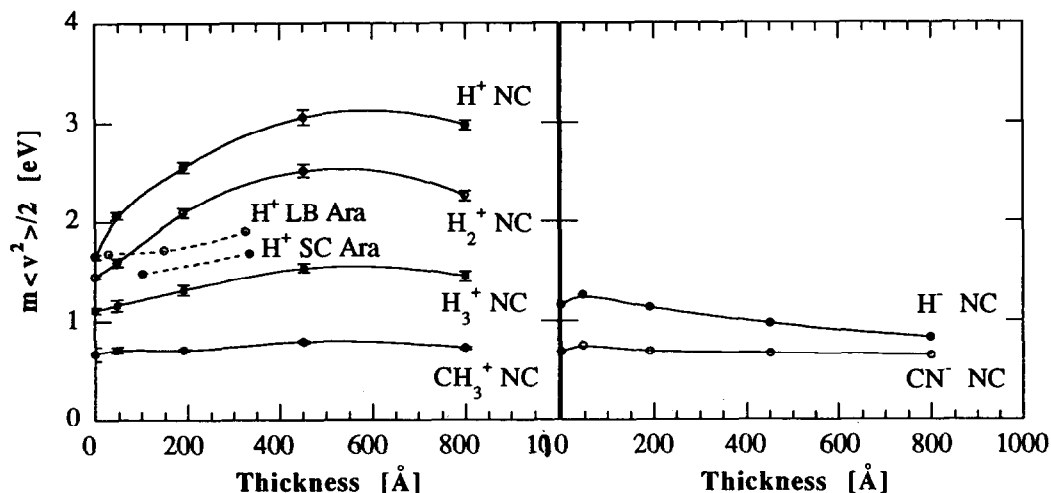


Fig. 3. The mean radial energy for a few fragment ions as a function of sample thickness for nitrocellulose (NC) films as well as for arachidic acid films prepared by spin coating (SC Ara) and the Langmuir-Blodgett technique (LB Ara).

## 4. Results

### 4.1. Experimental

**Spin coated nitrocellulose films:** The mean radial energy for different film thicknesses is presented in fig. 3. A broadening of the radial velocity distribution with increasing sample film thickness is observed for the positive hydrogen ions ( $H^+$ ,  $H_2^+$  and  $H_3^+$ ) and a slight narrowing is observed for the negatively charged hydrogen ion  $H^-$ . The heavier secondary fragment ions, i.e.  $CH_3^+$ ,  $H_2O^+$ ,  $H_3O^+$ ,  $NO^+$  and  $CN^-$  have radial velocity distributions which are independent of the sample thickness. An increase of the yield of  $H^+$  and a decrease of the yield of  $H^-$  as a function of sample thickness were observed (fig. 4a).

**Films of arachidic acid:** Independent of the method used for sample preparation, the radial velocity distribution of  $H^+$  changes only slightly as a function of film thickness as seen in fig. 3. This is contrary to what is observed for nitrocellulose. Also the yield of  $H^+$  and  $H^-$  for samples of spin coated arachidic acid is roughly constant (fig. 4b).

As reported earlier the dependence of the yield ( $Y$ ) of the positive hydrogen ions as a function of their mass ( $m$ ) follows an exponential law  $Y = a \exp(-bm^{1/2})$  [23]. From a fit of this expression to the data obtained, a value of  $b \approx 5 \text{ amu}^{-1/2}$  results, regardless of the sample type and its thickness. The absolute yield of  $H^+$  is of the order of 10%. The ratio of the absolute yield of  $H^-$  and  $H^+$  from the clean silicon substrate is  $\sim 0.9$  and for a thick (1400 Å) nitrocellulose film  $\sim 0.2$ .

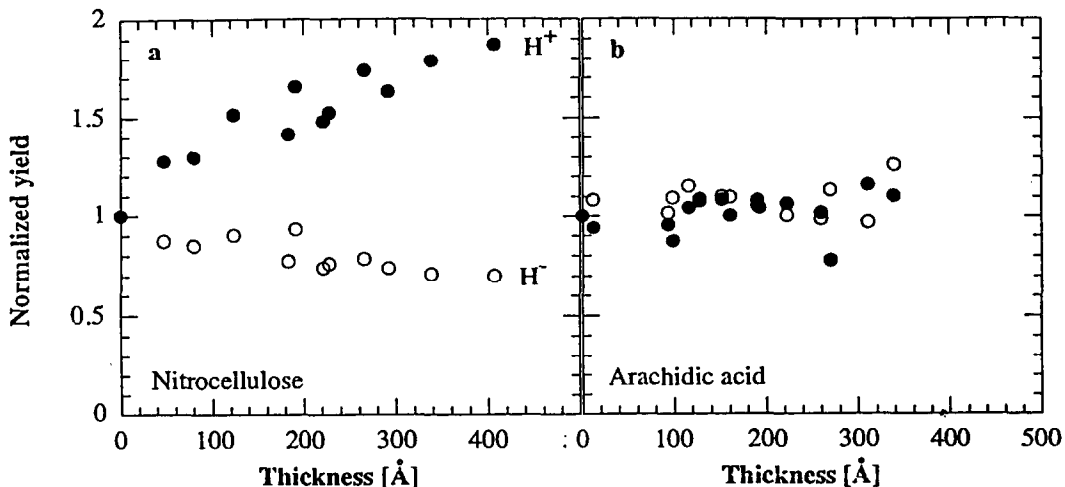


Fig. 4. The normalized yield of  $H^+$  and  $H^-$  as a function of sample thickness for films of (a) nitrocellulose and (b) arachidic acid bombarded by fission fragments from  $^{252}\text{Cf}$ .

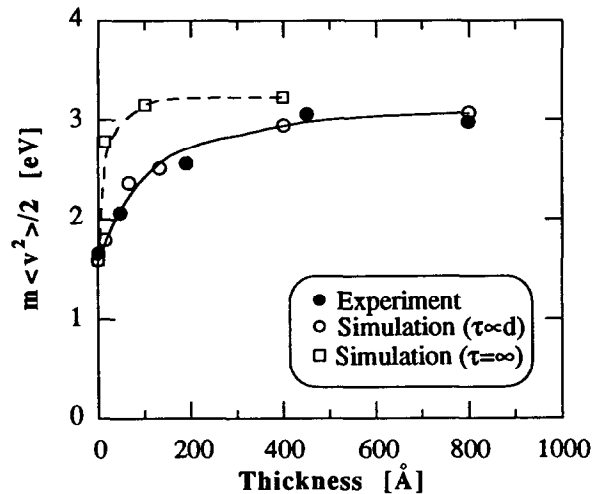


Fig. 5. The mean radial energy for  $H^+$  as a function of sample thickness for the neutralization time being infinite ( $\tau = \infty$ ) and proportional to the thickness ( $\tau \propto d$ ) compared with the experimental data for nitrocellulose films (fig. 3).

### 4.2. Simulations

The simulated mean radial energy of  $H^+$  as a function of sample thickness can be seen in fig. 5. The results are obtained using two different assumptions. In one case the neutralization time is assumed to be infinite. This assumption results in a much faster increase of the simulated mean radial energy than that of the experiments. In the second case the neutralization

time is assumed to be proportional to the sample thickness. The constant of proportionality was chosen to be  $1.3 \text{ \AA/fs}$  to give the best fit to the experimental data, which corresponds to e.g. a neutralization time of 300 fs for a sample thickness of 400  $\text{\AA}$ . This assumption gives a fair agreement with the experimental results on mean radial energy. The simulations give an increase in the relative yield by a factor of  $\sim 1.6$  when increasing the film thickness from zero to 400  $\text{\AA}$ . This is lower than the experimentally observed increase in relative yield of  $\sim 1.9$  (fig. 4).

## 5. Discussion

The fast increase of the width of the radial velocity distribution of  $\text{H}^+$  as a function of sample thickness obtained from the simulations using an infinite neutralization time shows that only the charges close to the surface contribute substantially to the acceleration (fig. 5). Consequently, the experimentally observed increase of the width of the radial velocity distribution with sample thickness cannot simply be attributed to the larger repulsion from a longer track. Simulations using a neutralization time proportional to the sample thickness, on the other hand, yield a fair agreement with the experiments. A thickness dependent neutralization time suggests that the neutralization of the charged track is dominated by electrons from the substrate.

The parameters of the simulations were determined to give *radial* velocity distributions which are consistent with the experimental data on thick films of nitrocellulose. Qualitatively, the dependence on sample thickness and neutralization time of the mean *axial* energy from the same simulations is similar. However, the magnitude of the simulated mean *axial* energy ( $\sim 5 \text{ eV}$ ) for a thickness of 400  $\text{\AA}$  is much smaller than experimentally measured:  $\sim 14 \text{ eV}$  [8],  $\sim 11 \text{ eV}$  [10], and  $8.0 \pm 0.2 \text{ eV}$  [11]. This discrepancy could be eliminated by including hydrogen ions with a higher initial kinetic energy as though they were formed for example in a two-electron process (e.g.  $-\text{C}-\text{H}^{2+} \Rightarrow -\text{C}^+ + \text{H}^+$ ). For a more complete description of the ejection process, collisions inside the solid also have to be taken into account. However, including these mechanisms would not change qualitatively the dependence of the radial and axial velocity distributions on sample thickness and track neutralization time.

The increase of the yield of  $\text{H}^+$  with sample thickness for the nitrocellulose films (fig. 4a) is reproduced qualitatively by the computer simulations. In the simulations the increase in yield is a consequence of the velocity dependent survival probability ( $p \propto \exp(-v_0/v_z)$ ). Ejection from a thicker film will result in a higher mean velocity normal to the sample surface and thus in a higher yield.

The radial velocity distribution of  $\text{H}^+$  from films of nitrocellulose shows a thickness dependence which is not observed with films of arachidic acid (fig. 3). This difference could be explained by the difference in structure and thus in conductivity between the highly excited part of the nitrocellulose and that of the arachidic acid films. A faster neutralization in the case of the arachidic acid films would lead to a smaller repulsion of the ejected  $\text{H}^+$  resulting in a lower mean energy (fig. 3). To explain why the velocity distribution of heavier ions is constant it could be argued that these are created at a later time and interact with a partially or totally neutralized track or that they are created further away from the ion trajectory than the positive hydrogen ions [5].

Gas phase collisions could, in principle, modify both yield and velocity distribution of ejected ions. A larger amount of material is ejected upon ion impact on thicker films [13] and the probability for gas collisions increases. This would, however, mainly affect the velocity distribution of the slower secondary ions rather than the fast hydrogen ions. Thus, the broadening of the radial velocity distribution of  $\text{H}^+$  as a function of sample thickness cannot be caused by changes in the probability for gas phase collisions with film thickness.

## 6. Conclusion

The width of the radial velocity distribution of the hydrogen ions is shown to increase with increasing sample thickness. Comparison is made with a very straightforward simulation of the Coulomb repulsion by the transiently ionized region where the track intersects the surface. The rough agreement indicates that the observed broadening of the radial velocity distribution of the positive hydrogen ions as a function of sample thickness can be attributed to repulsion from the track of positive charges created by the primary ion and neutralized by electrons mainly from the substrate. This indicates that measurements of positive light ions can be used to study the track neutralization process.

## Acknowledgements

The authors would like to thank R.E. Johnson, C.T. Reimann, A. Hedin and P. Demirev for many fruitful discussions. The Swedish National Board for Technical Development are gratefully acknowledged for financial support.

## References

- [1] K. Wien, *Radiat. Eff. Def. Solids* 109 (1989) 169.
- [2] B.U.R. Sundqvist, in: *Sputtering by Particle Bombard-*

- ment III, eds. R. Behrisch and K. Wittmaack (Springer, 1991) p. 257.
- [3] R.E. Johnson, *Int. J. Mass Spectrom. Ion Proc.* 78 (1987) 357.
- [4] E.F. da Silveira and E.A. Schweikert, *J. Chem. Phys.* 89 (1988) 6708.
- [5] K. Wien, O. Becker, W. Guthier, S. Della-Negra, Y. LeBeyec, B. Monart, K.G. Standing, G. Maynard and C. Deutsch, *Int. J. Mass Spectrom. Ion Proc.* 78 (1987) 273.
- [6] N. Fürstenau, W. Knippelberg, F.R. Krüger, G. Weiss and K. Wien, *Z. Naturforsch.* 32a (1977) 711.
- [7] O. Becker, *Nucl. Instr. and Meth.* 198 (1982) 53.
- [8] S. Widdiyasekera, P. Håkansson and B.U.R. Sundqvist, *Nucl. Instr. and Meth. B* 33 (1988) 836.
- [9] R. Moshhammer, R. Matthäus, K. Wien, Y. LeBeyec and G. Bolbach, *Proc. Ion Formation from Organic Solids (IFOS V)*, eds. A. Hedin, B.U.R. Sundqvist and A. Benninghoven (Wiley, Chichester, 1990) p. 17.
- [10] R.D. Macfarlane and D.L. Jacobs, *Proc. Ion Formation from Organic Solids (IFOS IV)*, ed. A. Benninghoven (Wiley, Chichester, 1989) p. 71.
- [11] R. Moshhammer, Thesis, Institute of Nuclear Physics, Technische Hochschule Darmstadt, Germany (1991).
- [12] R. Matthäus, Thesis, Institute of Nuclear Physics, Technische Hochschule Darmstadt, Germany (1992).
- [13] G. Säve, P. Håkansson, B.U.R. Sundqvist and U. Jönsson, *Nucl. Instr. and Meth. B* 26 (1987) 571.
- [14] G. Säve, P. Håkansson, B.U.R. Sundqvist, E. Söderström, S.E. Lindqvist and J. Berg, *Int. J. Mass Spectrom. Ion Proc.* 78 (1987) 259; *Appl. Phys. Lett.* 51 (1987) 1379.
- [15] R.M.A. Azzam and N.M. Bashara, *Ellipsometry and Polarized Light* (North Holland, Amsterdam, 1977).
- [16] R. Erlandsson, D. Fenyö, P. Håkansson and B.U.R. Sundqvist, unpublished results.
- [17] B. Sundqvist and R.D. Macfarlane, *Mass Spectrom. Rev.* 4 (1985) 421.
- [18] D. Fenyö, A. Hedin, P. Håkansson and B.U.R. Sundqvist, *Int. J. Mass Spectrom. Ion Proc.* 100 (1990) 63.
- [19] *Handbook of Chemistry and Physics*, 52th ed. (The Chemical Rubber Co., Ohio, 1971).
- [20] R. Stockbauer, E. Bertel and T.E. Madey, in: *Desorption Induced by Electronic Transitions I*, eds. N.H. Tolk, M.M. Traum, J.C. Tully and T.E. Madey (Springer, Berlin, 1983) p. 267.
- [21] R. Stockbauer, E. Bertel and T.E. Madey, *J. Chem. Phys.* 76 (1982) 5639.
- [22] J.C. Tully, in: *Desorption Induced by Electronic Transitions I*, eds. N.H. Tolk, M.M. Traum, J.C. Tully and T.E. Madey (Springer, Berlin, 1983) p. 31.
- [23] F. Riggi, *Nucl. Instr. and Meth. B* 43 (1989) 520.